

## Synthesis and structure of $W_3S_4Cl_4$

P. E. Rauch and F. J. DiSalvo

*Department of Chemistry, Cornell University, Ithaca, NY 14853 (USA)*

W. Zhou, D. Tang and P. P. Edwards\*

*Department of Chemistry, Cambridge University, Cambridge CB2 1EP (UK)*

(Received September 19, 1991; in final form October 10, 1991)

### Abstract

The synthesis of  $W_3S_4Cl_4$ , a layered tungsten thiohalide with a basic structure similar to  $TiS_2$  is described.  $W_3S_4Cl_4$  was synthesized from  $WCl_2$  and sulfur at 350 °C. The X-ray powder diffraction pattern was completely indexed on a small hexagonal unit cell with  $a = 3.336(1) \text{ \AA}$  and  $c = 5.907(1) \text{ \AA}$ . Electron diffraction studies revealed a  $4 \times 4 \times 8$  supercell, giving the compound a superstructure with  $a = 13.356 \text{ \AA}$  and  $c = 47.29 \text{ \AA}$ . An ordering of the tungsten vacancies which can account for this superstructure is discussed in light of the electron diffraction patterns.

### 1. Introduction

The synthesis of a new compound  $W_3S_4Cl_4$  was recently reported by Saito *et al.* [1]. Only the X-ray powder diffraction pattern and stoichiometry were given in the report. Because of our interest in transition metal sulfides, especially reduced early transition metal sulfides that form metal–metal bonded clusters, we became interested in investigating the synthesis and structure of this new compound. With the given stoichiometry, we believed that the compound might form a potential precursor to the yet unreported tungsten Chevrel phase  $M_xW_6S_8$  by reduction with a metal such as copper or indium.

The original X-ray powder diffraction pattern of  $W_3S_4Cl_4$  was indexed on the basis of a large rhombohedral cell [1] with  $a = 11.560(2) \text{ \AA}$  and  $c = 7.319(2) \text{ \AA}$  (hexagonal setting). After synthesizing  $W_3S_4Cl_4$  and studying its powder diffraction pattern, it became apparent that the compound was related to the layered dichalcogenides, probably having a structure related to that of  $CdI_2$ . In fact, the pattern was completely indexed on a smaller hexagonal cell ( $a = 3.336(1) \text{ \AA}$  and  $c = 5.907(1) \text{ \AA}$ ). Although all attempts to synthesize a  $M_xW_6S_8$  phase from  $W_3S_4Cl_4$  were unsuccessful, the compound proved interesting in its own right.

There are a number of halides, chalcogenides and halide–chalcogenides that have layered structures related to the  $CdI_2$  structure. Transition metal

---

\*Present address: The School of Chemistry, University of Birmingham, Edgbaston, Birmingham B15 2TT, UK.

dichalcogenides ( $\text{MX}_2$ ) can be viewed as close-packed layers of chalcogens (X) with transition metals filling holes between half of the layers. The two main differences between the structures of these compounds are (1) the coordination of the metal by the chalcogens is either octahedral or trigonal prismatic and (2) the stacking of the  $\text{MX}_2$  layers. In the case of transition metal dichalcogenides with a  $d^0$ ,  $d^3$  or  $d^4$  transition metal, such as  $\text{TiS}_2$  or  $\text{ReS}_2$ , octahedral coordination of the transition metal is observed. With  $d^1$  or  $d^2$  transition metal dichalcogenides such as  $\text{WS}_2$ , trigonal prismatic coordination is observed. There are exceptions to this situation, but in general these guidelines hold true [2].

Many transition metal dihalides have layered structures related to that of  $\text{CdI}_2$ . For example, most of the 3d transition metal dichlorides, dibromides and diiodides have layered  $\text{CdI}_2$  and  $\text{CdCl}_2$  structures in which the transition metal atoms occupy the octahedral holes. In addition,  $\text{Nb}_3\text{I}_8$  and  $\text{Nb}_3\text{Br}_8$  have layered structures [2, 3] where only three quarters of the octahedral holes between the alternate layers are occupied. In these compounds the metal atoms bond together to form trimers; consequently, the metal atoms do not sit at the center of the octahedron and the halide layers buckle to accommodate the metal displacements. Solid solutions between  $\text{Nb}_3\text{I}_8$  and  $\text{Nb}_3\text{Br}_8$  have similar structures [4], although the position of the metal trimers is disordered between the different layers. A few thiohalides have layered structures.  $\text{InSCl}$  and  $\text{InSBr}$  appear to have a  $\text{CdCl}_2$  structure, with the sulfur and chlorine randomly mixed in close-packed layers [3, 4].

## 2. Experimental details

### 2.1. Synthesis

The starting materials,  $\text{WCl}_6$  (99.99% metals purity, Strem Chemical Co., Newburyport, MA), 12 micron tungsten metal powder (99.9% purity, Aldrich Chemical Co., Milwaukee, WI) and sulfur (99.9999% purity, Atomergic, Plainview, NY) were used as received. As both 12 micron tungsten metal powder and  $\text{WCl}_6$  are air sensitive, they were handled in a glove box under inert atmosphere.

$\text{WCl}_2$  was synthesized by the reduction of  $\text{WCl}_6$  using tungsten metal powder in a quartz reaction tube [5]. Typically, 24 g (0.06 mol) of  $\text{WCl}_6$  and an excess 25 g (0.14 mol) of 12 micron tungsten powder were loaded into the quartz reaction tube (33 cm long, 25 mm O.D. and a wall 3 mm thick with a slight bend (about  $30^\circ$ ) 13 cm from the sealed end) under an argon atmosphere. After sealing under vacuum, the tube was placed in a furnace, leaving about 6 cm of the empty end of the tube outside the furnace and the newly sealed end containing the reactants inside the furnace. The  $\text{WCl}_6$  was then sublimed to the outside end of the tube by raising the internal temperature to  $270^\circ\text{C}$  for 30 min. The internal temperature was then raised to  $750^\circ\text{C}$  so that the  $\text{WCl}_6$  began refluxing. After a total reaction time of 14 h the reaction was essentially complete. At this point, the tube was allowed

to cool before being reinserted into the furnace with the  $\text{WCl}_2$  inside and the unreacted tungsten metal outside. The furnace was then heated to 450 °C for 2 h to sublime out any  $\text{WCl}_4$  or  $\text{WOCl}_4$  that may have contaminated the  $\text{WCl}_2$ , having formed as a byproduct ( $\text{WCl}_4$ ) or by reaction with the quartz tube ( $\text{WOCl}_4$ ).

The impure  $\text{WCl}_2$  was recrystallized from 100 ml of boiling 6 M HCl, and the solution cooled to -10 °C to obtain yellow-green needles of  $(\text{H}_3\text{O})_2\text{W}_6\text{Cl}_{14} \cdot 6\text{H}_2\text{O}$ . Pure  $\text{WCl}_2$  was obtained by heating the hydrate to 450 °C under a dynamic vacuum, heating at 100 °C  $\text{h}^{-1}$ . A final yield of about 25% was obtained based on the amount of  $\text{WCl}_6$  used.

$\text{W}_3\text{S}_4\text{Cl}_4$  was synthesized from  $\text{WCl}_2$  (4.1 g, 0.016 mol) and sulfur (3.3 g, 0.013 mol, as  $\text{S}_8$ ) sealed under vacuum in a Pyrex tube (approx. 20 cm long, 12 mm O.D., and a wall 2 mm thick with a bend near the middle). The reaction tube was placed in a two-zone furnace. The end of the tube containing the  $\text{WCl}_2$  and sulfur was kept at 350 °C, whilst the other end was kept at 200 °C to condense the excess  $\text{S}_2\text{Cl}_2$  byproduct. The reaction was completed in about 3 days; the end of the tube that had been kept at 200 °C was cooled in liquid nitrogen and sealed off to remove the  $\text{S}_2\text{Cl}_2$ . Any excess sulfur was removed by heating the sample to 200 °C under a dynamic vacuum. The compound was not treated as air sensitive. Elemental analysis (M-H-W Laboratories, Phoenix, AZ) gave 16.05% sulfur and 16.67% chlorine, a composition consistent with  $\text{W}_3\text{S}_4\text{Cl}_4$  containing about 5 wt.% of  $\text{WS}_2$  (see Section 2.2.). The expected analysis for pure  $\text{W}_3\text{S}_4\text{Cl}_4$  was sulfur, 15.61% and chlorine, 17.260%. If we now assume that the actual composition also contains exactly 4.5 wt.%  $\text{WS}_2$ , then the expected analysis is sulfur, 16.07% and chlorine, 16.48%.

## 2.2. Diffraction

All X-ray powder diffraction patterns were taken on an XDS 2000 powder diffractometer (Scintag Inc., Santa Clara, CA) using Cu  $K\alpha$  radiation. Table 1 lists the intensities and  $2\theta$  values observed by Saito *et al.* [1] and the results of our indexing of the X-ray powder diffraction pattern. Our X-ray powder diffraction pattern was essentially identical to Saito's (see Fig. 1). X-ray diffraction showed the compound to contain a small amount (about 5%) of an impurity, probably  $\text{WS}_2$ , characterized by a single diffraction peak at 14.39° ( $2\theta$ ). Electron diffraction studies were performed on a Jeol JEM-200CX electron microscope operating at 200 kV where a  $\pm 45^\circ$  double tilt specimen stage was used.

## 3. Results and discussion

In the original synthesis of  $\text{W}_3\text{S}_4\text{Cl}_4$ , a mixture of  $\text{WCl}_2$  and sulfur was heated to 350 °C in a sealed tube. Explosions occurred consistently when we followed this procedure. We also discovered that this reaction only produced a very poorly crystallized  $\text{WS}_2$  when carried out in an open system.

TABLE 1  
X-ray diffraction data for  $W_3S_4Cl_4$  [1]

$2\theta$ (obs)	$2\theta$ (calc)	$hkl$	Intensity (obs)
14.97	14.98	001	100
30.24	30.23	002	5
30.94	30.93	100	19
34.54	34.53	101	45
43.80	43.80	102	24
46.06	46.06	003	7
55.00	55.01	110	12
56.52	56.51	103	15
57.36	57.35	111	7
62.87	62.88	004	3
66.61	66.59	201	7
71.75	71.72	104	3
72.79	72.83	202	7

Hexagonal unit cell:  $a=3.336(1)$  Å and  $c=5.907(1)$  Å.

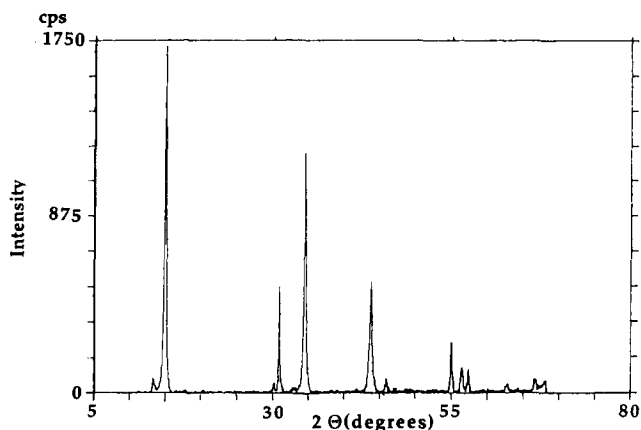


Fig. 1. The X-ray diffraction pattern of  $W_3S_4Cl_4$  (the weak impurity peak at  $14.39^\circ$  should be noted).

This led us to believe that an over pressure of  $S_2Cl_2$  was crucial for the synthesis of  $W_3S_4Cl_4$ , and hence a reservoir of  $S_2Cl_2$  was maintained at a reasonable pressure by the use of the  $200^\circ C$  zone in the two-zone furnace.

Another interesting feature of this synthesis was the interplay of time and reaction temperature.  $W_3S_4Cl_4$  did not form below  $310^\circ C$  or above  $400^\circ C$ . When the reaction was carried out at  $310^\circ C$  for 3 days, a less well-crystallized (intensity of all diffraction peaks, except the first, were reduced by 90%), but impurity free (by X-ray diffraction), compound formed. When the phase was synthesized in this way it did not diffract an electron beam. If the reaction was carried out at  $350^\circ C$  for 3 days, a well-crystallized phase that gave good X-ray and electron diffraction patterns was formed. Unfortunately, a small amount of an impurity was also found, as mentioned before,

characterized by a single X-ray diffraction peak at  $d=6.15 \text{ \AA}$  ( $2\theta=14.39^\circ$ ). Poorly crystallized  $\text{WS}_2$  may account for the impurity diffraction peak, consistent with the fact that  $\text{WS}_2$  formed at such a low temperature by vacuum decomposition of  $\text{W}_3\text{S}_4\text{Cl}_4$  is amorphous, or very poorly crystallized. If a higher reaction temperature or long reaction time was used, increasing amounts of this impurity were formed. Also, we have not been able to synthesize an impurity free phase that is both well crystallized and does not contain any of this impurity. In addition, it should be noted that the elemental analysis was consistent with a small amount (approx. 4.5 wt.%) of  $\text{WS}_2$ .

The X-ray powder diffraction pattern can be completely indexed on a hexagonal unit cell. However, such a small unit cell volume could contain a maximum of three atoms. In analogy to  $\text{TiS}_2$ , which has  $a=3.407 \text{ \AA}$  and  $c=5.695 \text{ \AA}$  [2], we might expect one tungsten atom, one sulfur atom and one chlorine atom in such a cell. Taken together with the graphite-like mechanical properties of this compound, we believe  $\text{W}_3\text{S}_4\text{Cl}_4$  has a structure similar to that of a layered dichalcogenide. In addition, because the compound only has a single anion–metal–anion layer repeat distance, the tungsten atoms must occupy octahedral holes, assuming close-packed anions. The structure appears to be that of  $\text{CdI}_2$ , in the space group  $P\bar{3}m1$  (No. 164), although the stoichiometry is not consistent with this assignment unless 25% of the tungsten sites are vacant. If there is no order among these tungsten vacancies, we would expect to see the observed X-ray diffraction pattern. As sulfur and chlorine have very similar scattering powers we cannot easily tell if these atoms are ordered. Although there are examples of both these phenomena in layered compounds (*i.e.* solid solutions of  $\text{Nb}_3\text{I}_8$  and  $\text{Nb}_3\text{Br}_8$  for metal vacancy disorder [4] and  $\text{InSCl}$  for sulfur chlorine disorder [3]) we decided to examine  $\text{W}_3\text{S}_4\text{Cl}_4$  by electron diffraction to see if there were any weak superstructure reflections that had been missed by X-ray diffraction. We anticipated that the  $\text{W}^{4+}-\text{W}^{4+}$  interactions might be strong, leading to an ordered state.

Figure 2 shows five electron diffraction patterns of  $\text{W}_3\text{S}_4\text{Cl}_4$ , the first four of which are generated by successive rotation about the reciprocal lattice vector  $[1\ 0\ 0]$ . These patterns are obtained with the electron beam parallel to the five directions;  $[0\ 2\ \bar{1}]$ ,  $[0\ 3\ \bar{1}]$ ,  $[0\ 4\ \bar{1}]$ ,  $[0\ 6\ \bar{1}]$  and  $[2\ 2\ \bar{1}]$ . The strong spots fit the indexing of the basic cell. The weak spots correspond to a  $4 \times 4 \times 8$  superlattice based on the original subcell. This leads to a new hexagonal cell with  $a=13.356 \text{ \AA}$  and  $c=47.29 \text{ \AA}$ . The reciprocal unit cell is shown in Fig. 3. Reciprocal lattice points with zero intensity are not shown. As the difference between the atomic numbers of sulfur and chlorine is only one, and any ordering between them will give extremely weak diffraction, we assume that the superlattice is primarily generated by ordering of the tungsten vacancies.

Next, a computer simulation of the diffraction patterns is used to model the tungsten vacancies. This model must not only give the correct diffraction patterns, but must also make sense chemically. Also, when given the choice of two equally good models, we choose the one of higher symmetry. This

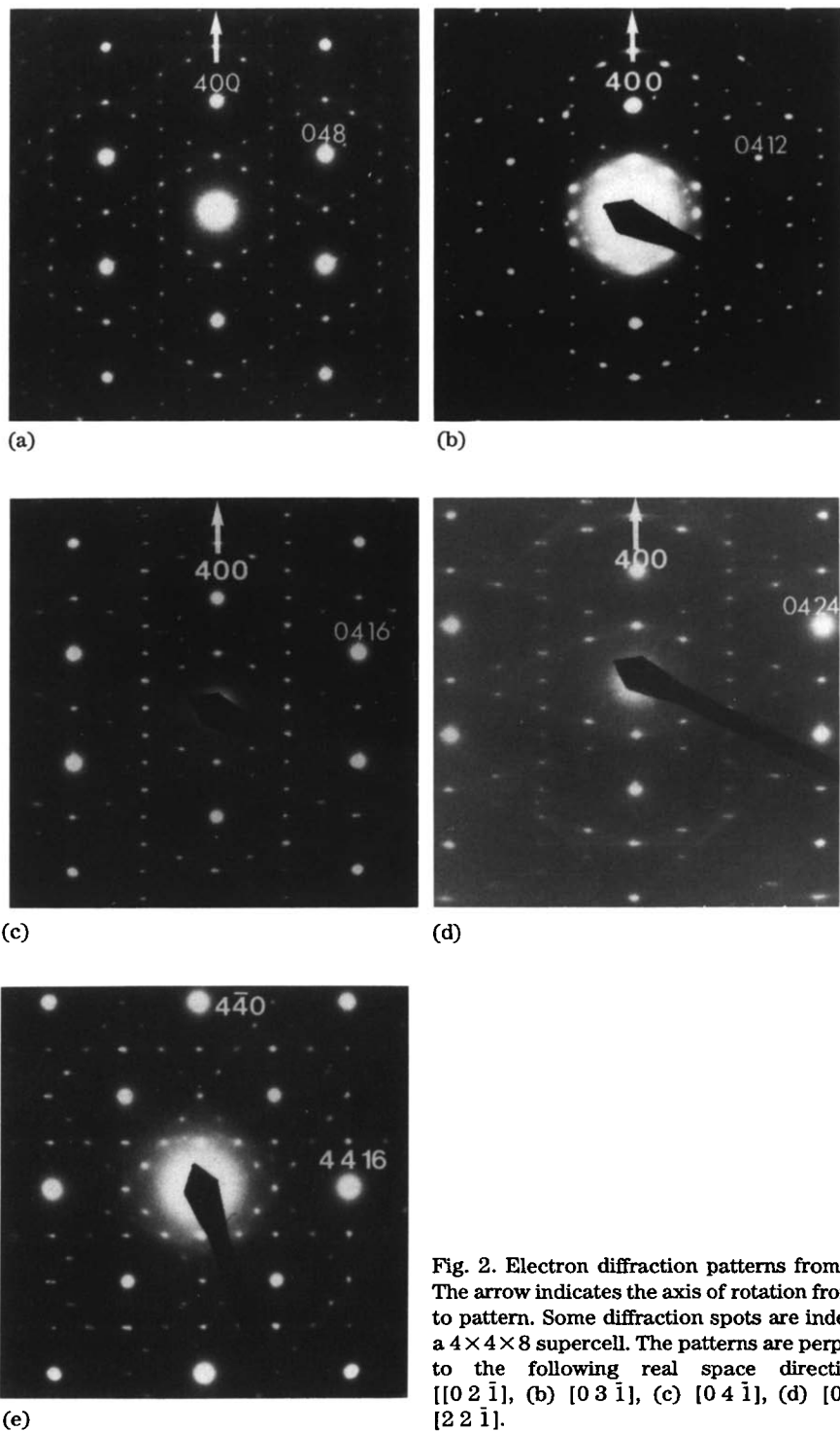


Fig. 2. Electron diffraction patterns from  $W_3S_4Cl_4$ . The arrow indicates the axis of rotation from pattern to pattern. Some diffraction spots are indexed onto a  $4 \times 4 \times 8$  supercell. The patterns are perpendicular to the following real space directions: (a)  $[0\ 2\ \bar{1}]$ , (b)  $[0\ 3\ \bar{1}]$ , (c)  $[0\ 4\ \bar{1}]$ , (d)  $[0\ 6\ \bar{1}]$ , (e)  $[2\ 2\ \bar{1}]$ .

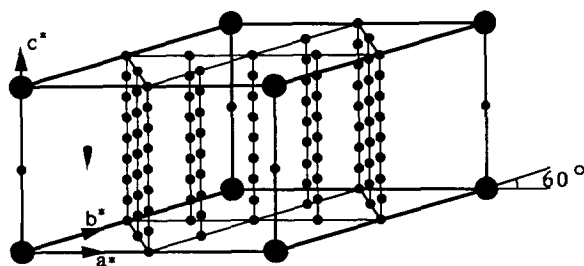


Fig. 3. The reciprocal unit cell for the substructure of  $W_3S_4Cl_4$  (outlined). The large dots represent strong reflections from the basic subcell. The smaller dots represent the positions of the observed weak reflections due to the superlattice.

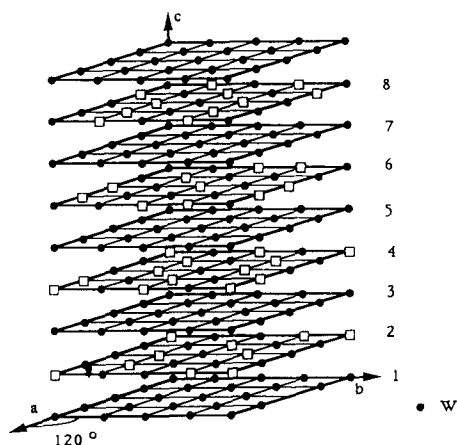


Fig. 4. The first tungsten vacancy model. The open squares represent tungsten vacancies and the black circles represent tungsten atoms. It should be noted that the third, fifth and seventh layers contain no tungsten vacancies.

is a trial and error method by which a structure is usually found, although this may not be the only reasonable solution to this problem [6]. In this study, only three of the many models tried are presented.

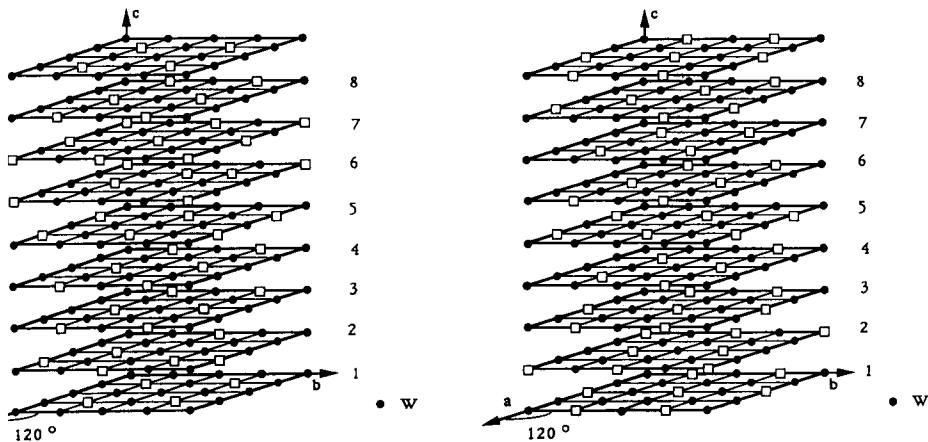
Figure 4 shows the first model. Only the tungsten layers are shown. This model has 28 tungsten vacancies (six in the second and sixth tungsten layers, eight in the fourth and eighth layers). This model could simulate all the diffraction patterns observed except that it has a major flaw; the vacancies are not evenly distributed between the layers. For example, there are no vacancies in the third layer, while in the two adjacent layers there are six or eight vacancies. Another flaw is that this model has 12.5% fewer vacancies than expected for a  $W_3S_4Cl_4$  stoichiometry.

Figure 5 shows the second model. This model has an equal number of vacancies in each layer, four, although they are not distributed in the same fashion within each layer. The four vacancies in the first, third, fifth and seventh layers, as well as in the fourth and eighth layers, form a rhomb within the layer, with a distance between tungsten vacancies of  $2a$  or more

where  $a$  is the first dimension of the original unit cell). The vacancies in the second and sixth form a smaller rhomb, with  $a$  the shortest distance between tungsten vacancies. The problem with this model is that the vacancies are not uniformly distributed in the  $ab$  plane. In addition, although this model could simulate the diffraction patterns along the five directions, the diffraction patterns along the equivalent directions  $[2\ 0\ \bar{1}]$ ,  $[3\ 0\ \bar{1}]$ ,  $[4\ 0\ \bar{1}]$  and  $[6\ 0\ \bar{1}]$  are different. Thus the symmetry of the supercell is less than trigonal.

Figure 6 shows the third and final model. The four tungsten vacancies in each layer form either a  $2a \times 2a$  rhomb or a  $2a \times \sqrt{3}a$  rectangle, hence they are more evenly distributed than in the second model. In addition, the reflection conditions for the diffraction spots with indices  $[hkl]$  and  $[\bar{h}\bar{k}\bar{l}]$  are the same, although their intensities need not be the same, giving the same diffraction pattern along equivalent directions. The only problem with this model is its symmetry. The vacancies either form rhombs or rectangles in each tungsten layer. A more symmetrical distribution could not be found that would reproduce all the observed diffraction patterns as well as this third model does. Therefore this model is accepted as the most plausible tungsten vacancy arrangement.

This final model is noteworthy in that the tungsten vacancies, though ordered, do not seem to lead to the formation of metal-metal clusters because superlattice peaks are all weak. In other compounds with similar stoichiometry, such as  $\text{Nb}_3\text{I}_8$ , the strong distortions from metal-metal clusters produce easily seen superlattice lines in X-ray diffraction [7].



5. The second tungsten vacancy model. The open squares represent tungsten vacancies and the black circles represent tungsten atoms. All layers contain tungsten vacancies. In the third and seventh layers the shortest distance between two vacancies is  $a$ , while in the other layers the distances between vacancies are not less than  $2a$ .

6. The third and final tungsten vacancy model. The open squares represent tungsten vacancies and the black circles represent tungsten atoms. In this model, vacancies form either rectangles that are  $2a \times \sqrt{3}a$ , or rhombs that are  $2a \times 2a$ .



Until now we have not considered the sulfur and chlorine atoms because their superstructure would diffract very weakly compared with the ordering of tungsten vacancies. Careful inspection of the diffraction pattern along the  $[03\bar{1}]$  (Fig. 2(b)) direction shows that the spots indexed as  $\pm(0\ 4\ 12)$  and  $\pm(4\ 4\ 12)$  are weaker than their counterparts in some of the other patterns, such as  $\pm(0\ 4\ 8)$  and  $\pm(4\ 4\ 8)$  in  $[0\ 2\ \bar{1}]$  (Fig. 2(a)). These spots are produced by the superstructure, although with the arrangement of tungsten vacancies in the third model their intensity would be zero. Only an ordering of the sulfur and chlorines would make these spots visible. The arrangement that gives rise to the largest intensity of these spots is for layers of sulfur or chlorine to come in pairs, or looking along the  $c$ -axis, the layer sequence would be tungsten–chlorine–chlorine–tungsten–sulfur–sulfur–tungsten. This arrangement does not produce spots as intense as those observed, although this could be as a result of errors from the dynamic calculation or inaccuracy of the sulfur and chlorine positions along the  $c$ -axis. In other superstructures involving sulfur and chlorine these spots are weaker, if not absent, contrary to the experimental results.

Figure 7 shows the simulated diffraction patterns created by the third arrangement of tungsten vacancies, along with proposed ordering of the sulfur and chlorine atoms. This simulation is almost identical to the observed

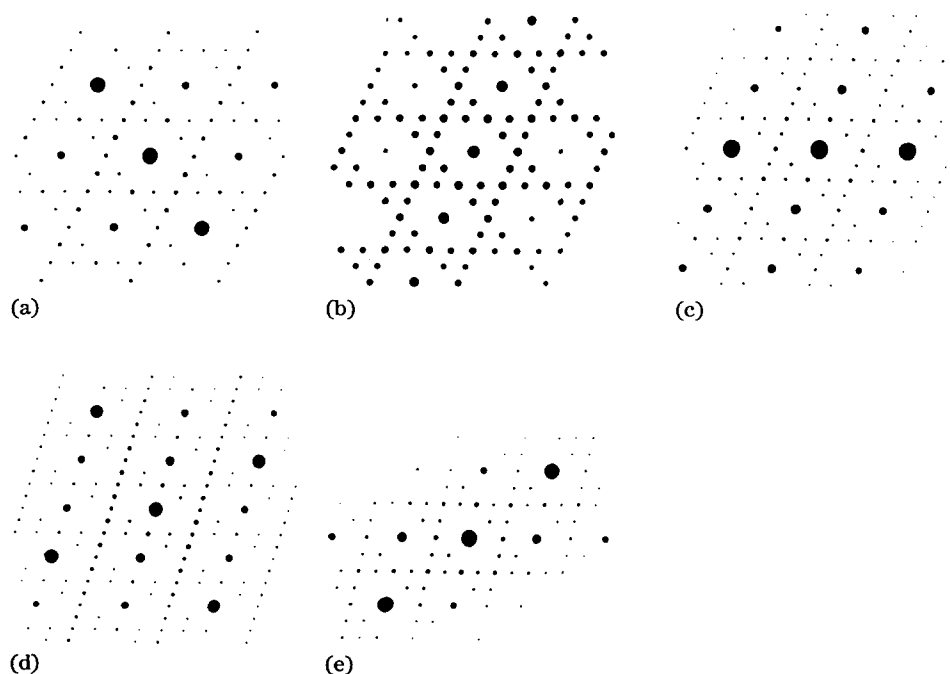


Fig. 7. Simulated electron diffraction patterns of  $W_3S_4Cl_4$ . Some diffraction spots are indexed. The patterns are along the following directions: (a)  $[0\ 2\ \bar{1}]$ , (b)  $[0\ 3\ \bar{1}]$ , (c)  $[0\ 4\ \bar{1}]$ , (d)  $[0\ 6\ \bar{1}]$ , (e)  $[2\ 2\ \bar{1}]$ .

diffraction patterns. While this suggests some sulfur/chlorine ordering, it relies on the final model of tungsten vacancies being correct.

An impurity phase, identified by its needle-like morphology, was also found in our samples of  $W_3S_4Cl_4$ . An energy dispersion spectrum (EDS) showed this new compound to be tungsten rich. Using the  $W_3S_4Cl_4$  as an internal standard, the stoichiometry of this new phase was approximately  $W_{4.45}S_4Cl_4$ . The electron diffraction pattern shown in Fig. 8 allowed this phase to be indexed on an orthorhombic cell with  $a=3.25$  Å,  $b=3.73$  Å and  $c=12.1$  Å; a structure not related to that of the majority phase. As the total weight percent tungsten in the sample (obtained from chemical analysis by difference) is off by less than 1%, assuming a 4.5%  $WS_2$  impurity, this phase must be a very small percentage of the original material. This is consistent with the observation that only a few small needles are seen attached to plates of  $W_3S_4Cl_4$ .

An interesting feature of this orthorhombic tungsten thiochloride can be seen in the electron diffraction patterns. Parallel lines running in the same direction are present in all of the diffraction patterns. This indicates the presence of diffuse sheets of intensity in reciprocal space. These lines probably correspond to a well ordered three-dimensional framework containing positionally disordered atoms in parallel one-dimensional channels within the framework.

#### 4. Conclusion

A new layer transition metal compound,  $W_3S_4Cl_4$ , has been described. Although this compound was reported earlier, we report a more extensive characterization of the structure. This phase exists as a hexagonal layered compound, and the presence of  $S_2Cl_2$  vapor is important during its synthesis. In addition, the use of electron diffraction has allowed us to suggest possible models for the ordering of tungsten vacancies and also, possibly, for the ordering of sulfur and chlorine atoms. Finally, we also report a new orthorhombic tungsten thiochloride, found as an impurity in the  $W_3S_4Cl_4$  and characterized by electron diffraction and EDS.

#### Acknowledgments

The support from NATO for travel to England, the Department of Energy, Basic Energy Sciences (Grant No. DE-FG02-87ER45298), SERC and British Petroleum for the work at Cambridge are greatly appreciated.

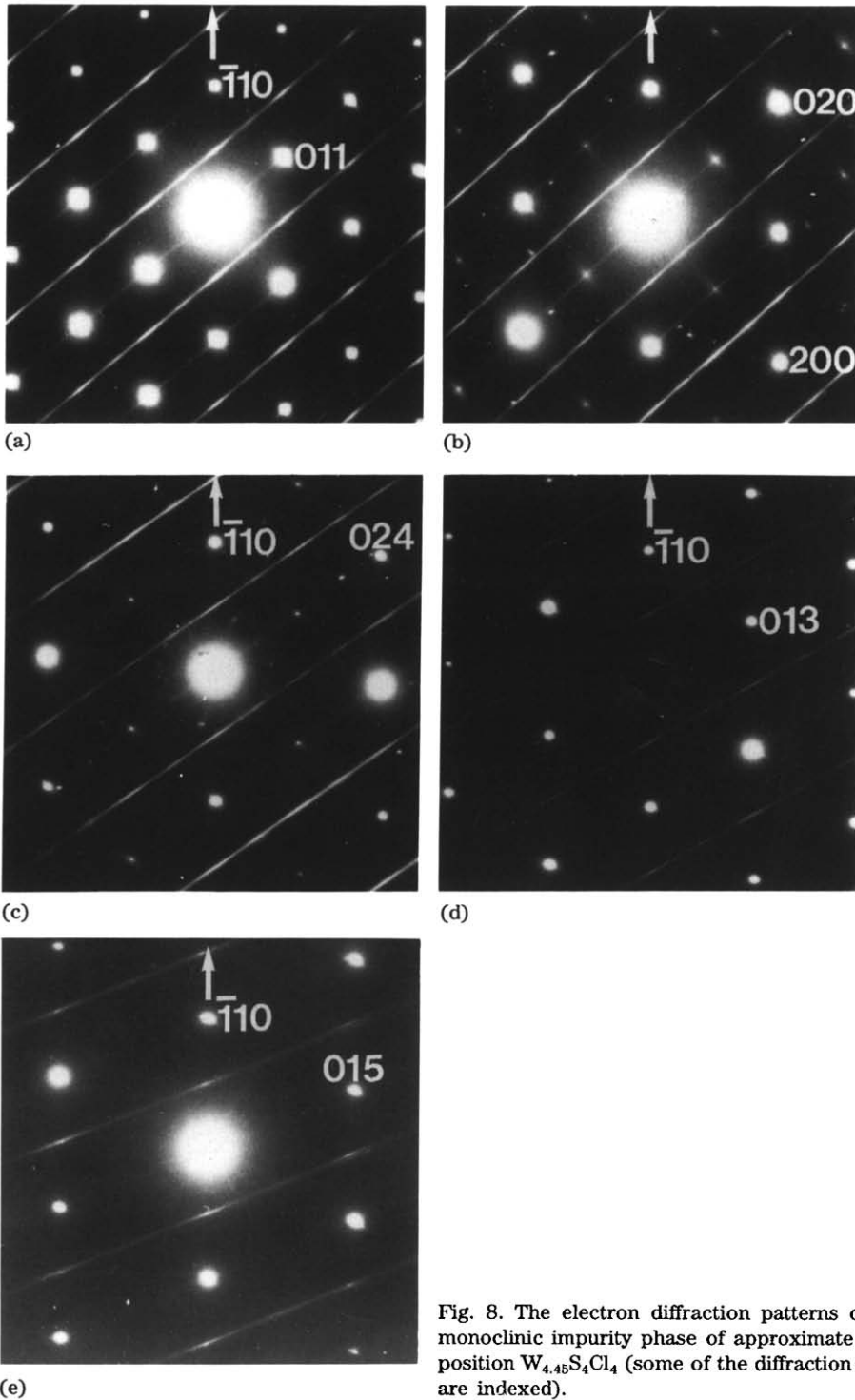


Fig. 8. The electron diffraction patterns of the monoclinic impurity phase of approximate composition  $W_{4.45}S_4Cl_4$  (some of the diffraction spots are indexed).

**References**

- 1 T. Saito, A. Yoshikawa, T. Yamagata, H. Imoto and K. Unoura, *Inorg. Chem.*, **28** (1989) 3588.
- 2 F. Lévy (ed.), *Crystallography and Crystal Chemistry of Materials with Layered Structures*, Vol. 2, Reidel, Dordrecht, 1976.
- 3 A. F. Wells, *Structural Inorganic Chemistry*, Clarendon Press, Oxford, 1984.
- 4 A. Simon, personal communication, 1991.
- 5 G. M. Ehrlich, P. E. Rauch and F. J. DiSalvo, submitted to *Inorg. Synth.*.
- 6 D. Tang, W. Zhou and D. A. Jefferson, to be published.
- 7 A. Simon and H. G. von Schnering, *J. Less-Common Met.*, **11** (1966) 31.